

DOE NETL: 30 October 2023

Computational Analysis of Thermal Management of Next Generation Gas Turbines

Tom I-P. Shih

School of Aeronautics and Astronautics, Purdue University

Mark Bryden

Ames National Laboratory, U.S. Dept. of Energy

Richard Dalton

National Energy Technology Laboratory, U.S. Dept. of Energy

Acknowledgement: NETL: Doug Straub & Justin Weber
Purdue: Jay Kim, Chien-Shing Lee, Sabina Nketia, Adwiteey Shishodia



Our nation's goal to reach 100% carbon-free electricity by 2035 opens many challenges and opportunities for gas turbines.

There are many pathways to transition from what we have today to one that is 100% carbon free!

For the gas-turbine hot section:

- Need to continue pushing the limits of
 - all technologies: combustion, aerothermal, materials, control
 - all fuels: NG, NG + H₂, H₂, ammonia, ammonia + H₂, sCO₂, ...
for reliable operation, increased efficiency, and increased service life.
- **On GT aerothermal**, the need – for any fuel – continues to be
 - Reducing aerodynamic loss for efficiency.
 - Reducing cooling flow for efficiency and service life.

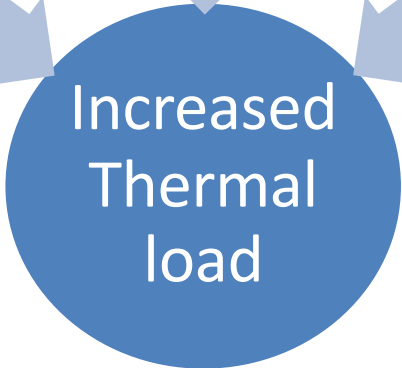
Challenges and Opportunities for Aerothermal



$H_2 \approx CH_4 / 3$
in energy density
higher volumetric flow rate to get same work output

- more H_2O
- H_2O more efficient than CO_2 on infrared radiation
higher gas radiation

H_2 has higher adiabatic flame temperature
higher temperature in hot-gas path

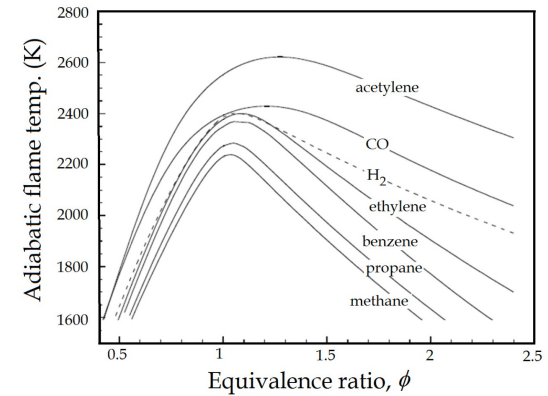


- Other Challenges:**
- cost of H_2 manufacture
 - infrastructure to transport and store H_2 .

Need new designs, which REQUIRE

- deep understanding of the fundamentals.
- better, faster, cheaper D&A tools.

This is the focus of our research!



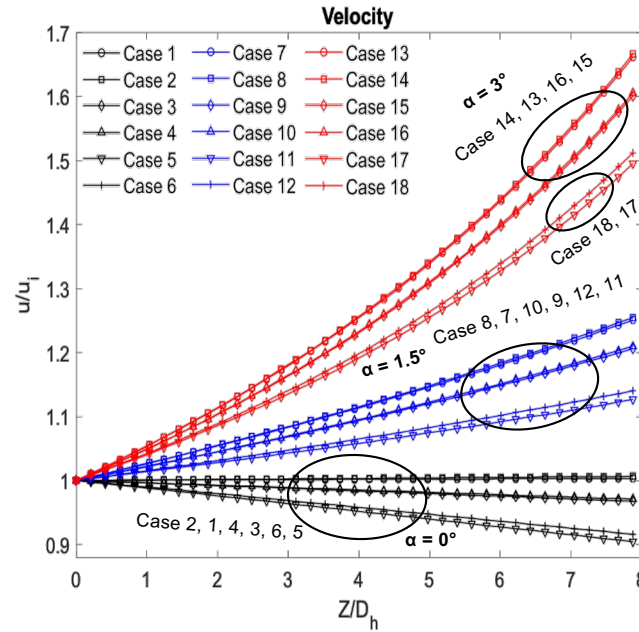
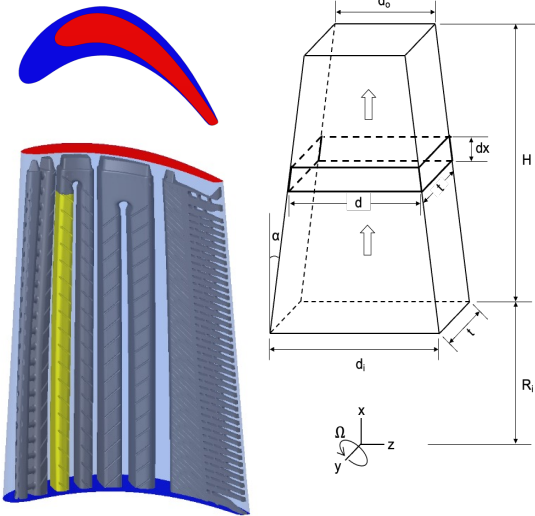
Jadidi, et al, Coatings, 2015

Current Efforts

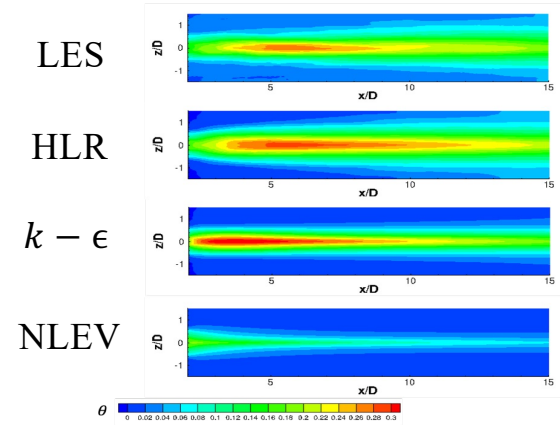
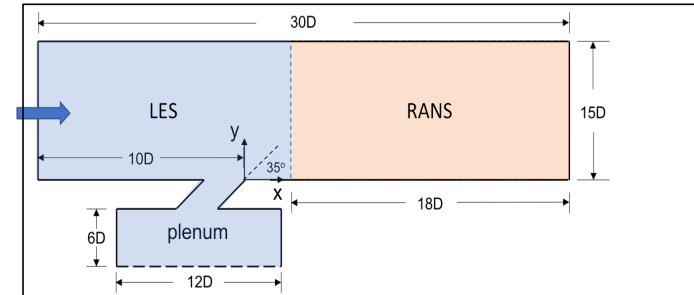
Tools

- Hybrid LES-RANS methods (2 papers in IJNMF - 2021 and 2022)
- ROM for internal cooling passage – tapered duct (2024 IGTI)
- ROM for vane and blade w/ internal and film cooling
- ROM + Optimization + machine learning for design (with Doug Straub and Justin Weber of NETL)

Fundamentals Applications



Max relative error in $\rho, V,$ and T are 4.9%, 7.1%, 0.9%, 4.7% for a ribbed duct.



The total number of cells reduced by 35% when compared to the LE. Cost was reduced by 57%.

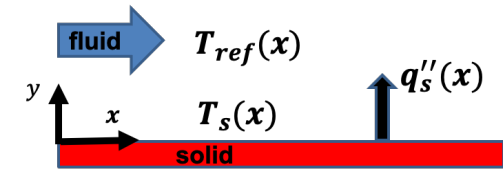
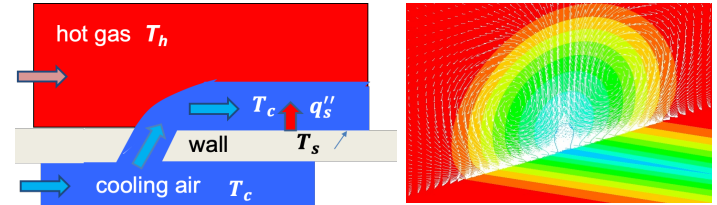
Current Efforts

Tools

Fundamentals:

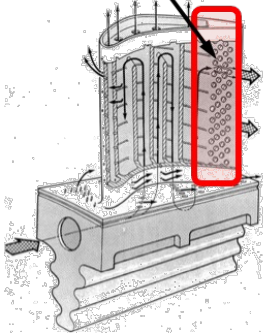
- Revisit $T_{adiabatic}$ on its physical meaning & how to measure.
- Scaling lab to engine conditions: (1) high heating loads ($T_w/T_b \approx 1$ in labs to T_w/T_b up to 2 in engines) and (2) rotation
- Revisit film cooling that couple the flow in the cooling passage and the hot-gas flow (2024 IGTI; with Doug Straub and Justin Weber of NETL)

Applications

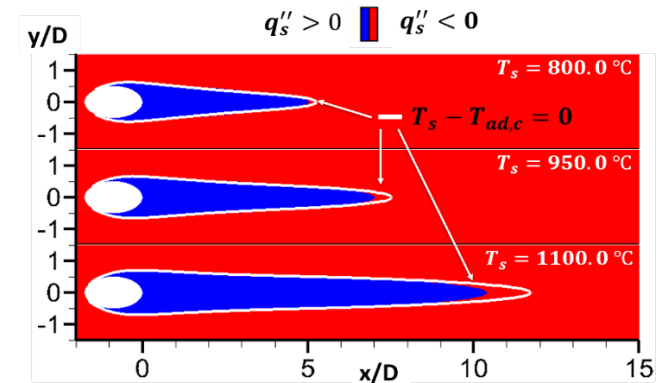
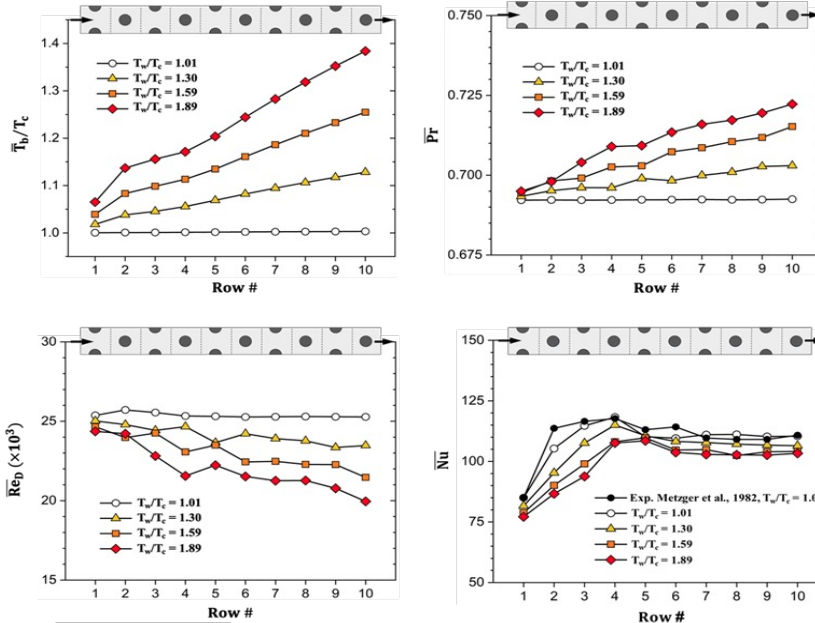


$$q''_s = h(T_s - T_{ref})$$

trailing-edge cooling
pin-fin array



IJHMT 2021



IGTI 2020

Current Efforts

Tools:

- Hybrid LES-RANS methods (2 papers in IJNMF - 2021 and 2022)
- ROM for internal cooling passage (2024 IGTI)
- ROM for vane and blade w/ internal and film cooling
- ROM + Optimization + machine learning for design

Fundamentals:

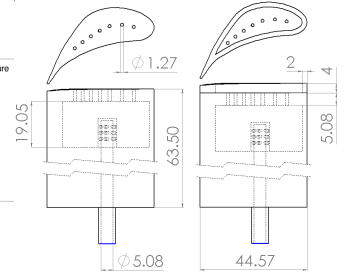
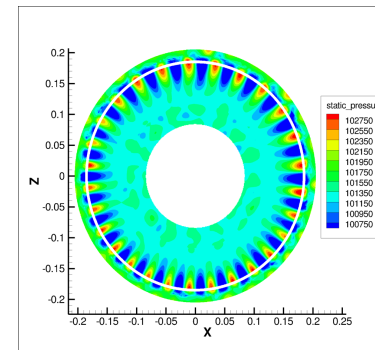
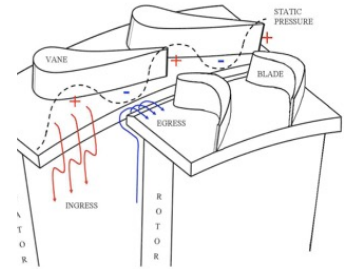
- Revisit $T_{adiabatic}$ on its physical meaning & how to measure.
- Scaling lab to engine conditions: (1) high heating loads (T_w/T_b bear 1 in labs to T_w/T_b up to 2 in engines) and (2) rotation
- Revisit film cooling that couple the flow in the cooling passage and the hot-gas flow (2024 IGTI)

Applications:

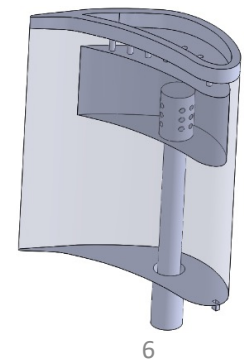
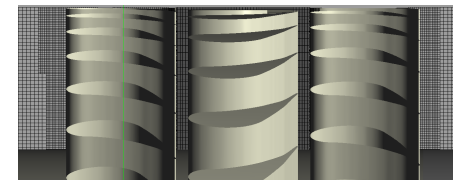
- Ingress/egress through rim seals via RANS & LES (2 papers in Energies)
- Blade-tip leakage in a 1.5 stage turbine via RANS & LES (2024 IGTI)
- Internal cooling w and w/o rotation and taper (2024 IGTI)
- New film-cooling holes: downstream VGs, Y-shaped hole
- New film-cooling design paradigms from machine learning

RIM SEALS: Bath and Aachen test rigs:

- rotation only
- rotation + vanes
- rotation + vanes & blades



BLADE TIP in 1.5 stage: flat, squealer, ... w/ and w/o film cooling



LES and RANS of Rotationally- and Externally-Induced Ingress in an Axial Seal of a Rotor-Stator Configuration

Purdue: Sabina Nketia and Tom I-P. Shih
DoE Ames Lab: Mark Bryden
DoE NETL: Richard Dalton and Rich Dennis

- Nketia, S., Shih, T.I-P., Bryden, K.M., Dalton, R., and Dennis, R., “Large-Eddy Simulation of Rotationally-Induced Ingress and Egress about an Axial Seal between Rotor and Stator Disks,” *Energies*, 2023, Vol. 16, 4354; DOI: <https://doi.org/10.3390/en16114354>.
- Nketia, S., Bryden, K.M., Dalton, R., and Shih, T.I-P., “Large-Eddy Simulation of Externally-Induced Ingress about an Axial Seal by Stator Vanes,” *Energies*, 2023, Vol. 16, No. 16,5985; DOI: <https://doi.org/10.3390/en16165985>.

Supported by the US Department of Energy-Office of Fossil Energy, Advanced Turbines Program under contract no. DE-AC02-07CH11358 through the Ames Laboratory agreement no. 26110-AMES-CMI.



U.S. DEPARTMENT OF
ENERGY



OUTLINE

- Introduction
- Literature Review
- Objective
- Problem Description
- Problem Formulation
- Numerical Method of Solution
- Verification and Validation
- Results
- Summary and Conclusions

Introduction

In gas turbines, all components exposed to hot gases must be cooled.

- Hot gas can be as hot as 2,000 °C.
- Best Ni-based superalloy used for blades, vanes, and endwalls can handle about 1,000 °C sustained temperature.
- Metal used to make rotor and stator disks can handle about 850 °C.

One region that needs attention is ingress into the wheelspace between the rotor and stator disks.

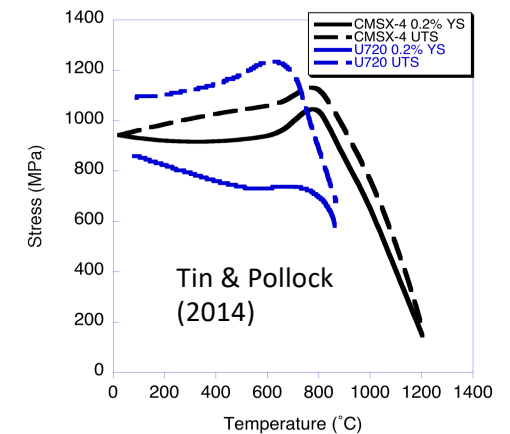
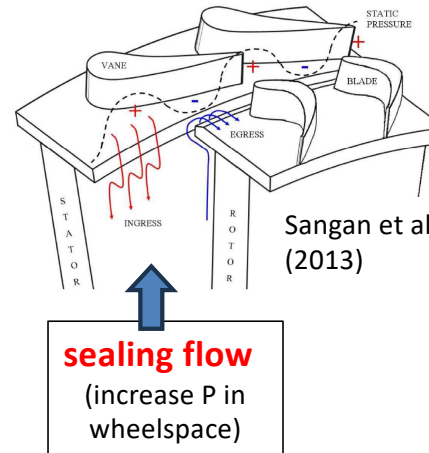
Rim seals and sealing flow are used to minimize ingress.

Sealing flow accounts for 1-2% of total flow through the HPC⁶, which is 6.66-13.3 % of the total cooling flow.

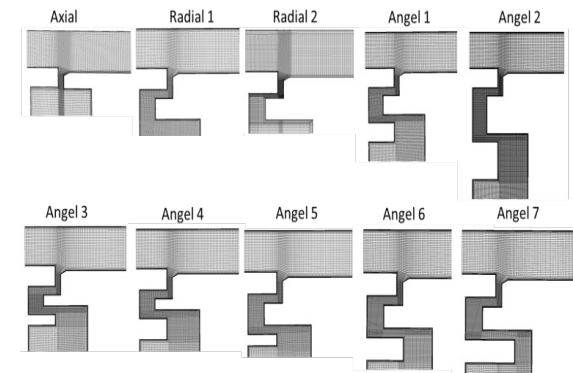
A 50% reduction in purge flow could

- increase efficiency of a 2-stage GT by 0.5%
- Reduce fuel consumption by 0.9%

Designs that minimize ingress require in-depth understanding of the fluid mechanics and how fluid flow and geometry affect ingestion.

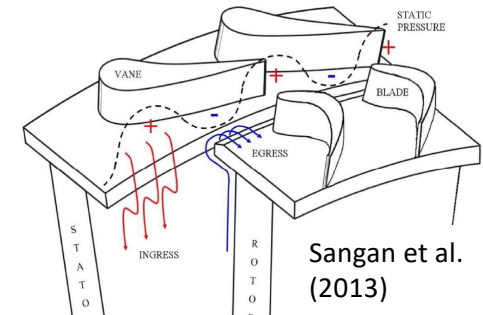


rim seals (increase discharge coefficient into wheelspace)



Previous Work on Rotationally- and Externally-Induced Ingress

Ingress is induced by: (1) **the rotor disk and its rotation (rotationally-induced ingress)**; (2) the pressure variation about the stator vanes' trailing edges, and (3) oscillations in the stagnation pressure created by the rotating blades.



rotationally-induced (RI) ingress

Experimental

- Phadke & Owen (1980, 1983, 1988a, 1988b, 1988c)
- Dadkhah et al. (1992)
- Bohn et al. (1995)
- Sangan et al. (2013b)

Computational

- Bohn et al. (1995)
- Cao et al. (2003)
- Jakoby et al. (2004)
- Boudet et al. (2005)
- Rabs et al. (2009)
- Gao et al. (2018)

externally-induced (EI) ingress

Experimental

- Green and Turner (1994)
- Bohn et al. (2003)
- Roy et al. (2005)
- Eastwood et al. (2012)
- Sangan et al. (2013)

Computational

- Bohn et al. (1995)
- Bohn et al. (1999)
- Roy et al. (1999)
- Bohn et al. (2000)
- Roy et al. (2001)
- Cao et al. (2004)
- Zhou et al. (2011)
- Roy et al. (2001)
- Johnson et al. (2009)
- O'Mahoney et al. (2011)
- Wang et al. (2012)
- Ding et al. (2013)
- Green et al. (2014)
- Liu et al. (2015)
- Chew et al. (2018)
- Hösgen et al. (2020)

Key Dimensionless Parameters

Nondimensional **sealing flow**, $c_W = \dot{m}_c / \mu_c r_o$

Reynolds number in annulus, $Re_{D_h} = (\rho_h V_h D_h) / \mu_h$

External Reynolds number, $Re_w = (\rho_h V_h r_o) / \mu_h$

Rotational Reynolds number, $Re_\phi = \rho_h \omega r_o^2 / \mu_h$

Ratio of external Re to rotational Re, $Re_w / Re_\phi = V_h / (\omega r_o)$

Coefficient of pressure on stator platform, $C_p = (P - \bar{P}) / (0.5 \rho \omega^2 r_o^2)$

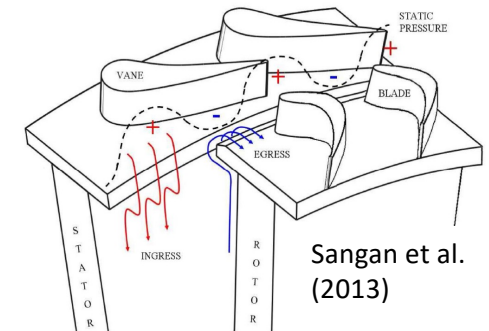
Sealing effectiveness, $\beta = (c_s - c_a) / (c_o - c_a)$

r_o is rotor hub; c is CO_2 concentration; ω is angular velocity of rotor
Subscripts: c – cold, h - hot

Key Findings and Gaps in Understanding

Overall:

- Ingress is induced by: (1) rotor disk and its rotation; (2) the pressure variation about the stator vanes' trailing edges, and (3) stagnation pressure induced by the rotor blades.
- Generating benchmark quality experimental data that can be used to validate CFD (Green et al. (2014). at OSU, Sangan et al. (2013) at Bath).
- If $Re_w/Re_\phi \ll 1 \rightarrow$ RI dominated; if $Re_w/Re_\phi \geq 1 \rightarrow$ EI dominated



RI Ingress

- Kelvin-Helmholtz instability identified (Rabs et al. (2009)), but how KHI affects RI ingress not explained.
- Alternating regions of high & low P on rotor-side of rim seal have been identified (Green et al. (2014)), but their causes have never been explained (effects of stator vane is only a part of the answer).
- Conflict flow trajectories in and out of the seal (Bohn et al. 1995, Sangan (2013)).
- RANS cannot predict RI ingress.
- LES studies done so far used coarse mesh (Gao et al. (2018)).

EI Ingress

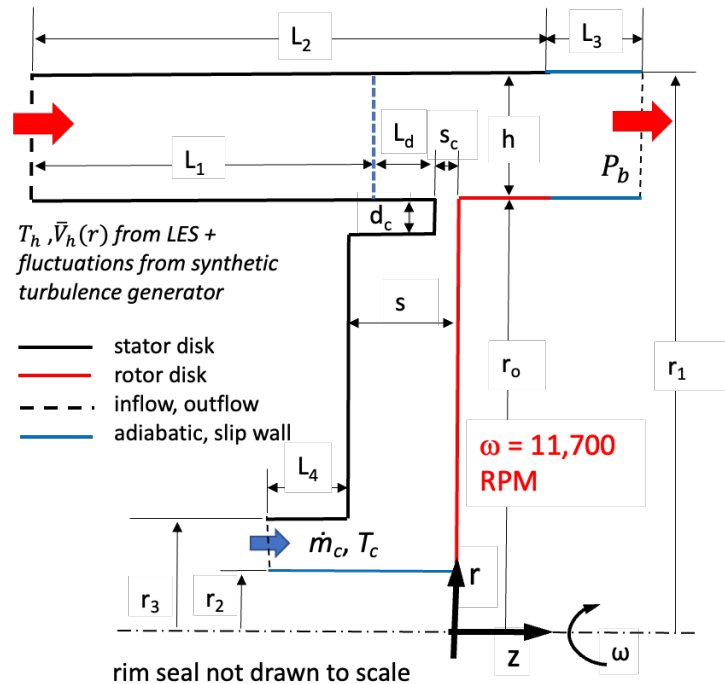
- $C_p = (P - \bar{P}) / (0.5\rho\omega^2 r_o^2)$ is deemed the predictor for EI ingress (Sangan et al. (2013) at Bath), but want to verify.
- Pressure induced by vane dominates ingress (Roy et al. (2001)), but want to understand effect of rotation.
- RANS cannot predict EI ingress. (Liu et al. (2015))
- LES studies done so far used coarse mesh. (O'Mahoney et al. (2011))

Objective

- Examine the flow mechanisms creating **rotationally-induced ingress** in a rotor-stator configuration **without vanes and without blades**
- Assess the accuracy of LES and RANS in predicting flow mechanisms creating **externally-induced ingress** by stator vanes in a rotor-stator configuration **with vanes and without blades**

Problem Description

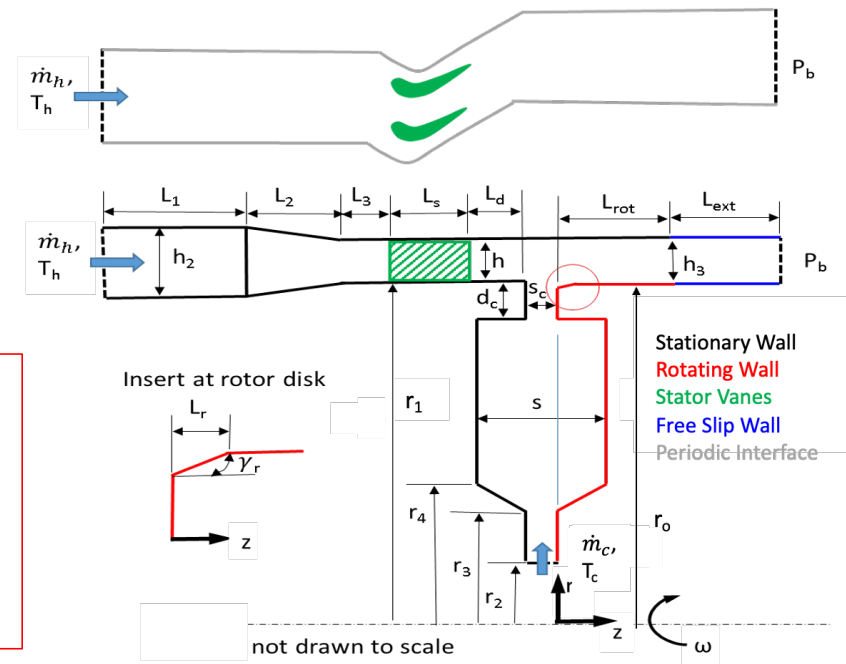
RI Ingress: no vanes & no blades (Aachen)



$r_0 = 116.25$ mm, $r_1 = 165.25$ mm, $s_c = 1.7$ mm, $d_c = 4.5$ mm, $L_1 = 150$ mm, $L_2 = 210.7$ mm, $L_3 = h$, $L_4 = 20$ mm, $L_d = 10$ mm, and $h = r_1 - r_0$

$c_w = \dot{m}_c / \mu_c r_0$	1000/0
$Re_{D_h} = (\rho_h V_h D_h) / \mu_h$	3.88×10^5
$Re_w = (\rho_h V_h r_0) / \mu_h$	0.46×10^6
$Re_\phi = \rho_h \omega r_0^2 / \mu_h$	1.13×10^6
$Re_w / Re_\phi = V_h / (\omega r_0)$	0.41

EI Ingress: vanes & no blades (Bath)



Sealing flow has 5% CO₂.
If no ingress, then CO₂ in wheelspace will be 5%.

$h_2 = 25$ mm, $h_3 = 11.233$ mm, $h = 10$ mm, $d_c = 5$ mm, $L_1 = 476$ mm, $L_2 = 94$ mm, $L_3 = 18$ mm, $L_s = 20.5$ mm, $L_d = 6$ mm, $L_r = 1.787$ mm, $L_{rot} = 50$ mm, $s_c = 2$ mm, $s = 20$ mm, $r_0 = 193.8$ mm, $r_1 = 195$ mm, $r_2 = 84.5$ mm, $r_3 = 116.64$ mm, $r_4 = 122$ mm, $\gamma_r = 24.89^\circ$, $\omega = 3,000$ RPM, $T_h = 23.34$ °C, $\dot{m}_h = 0.484$ kg/s, $P_b = 101,325$ Pa, $T_c = 23.34$ °C, $\dot{m}_c = 0.0068$ kg/s.

$c_w = \dot{m}_c / \mu_c r_0$	2000
$Re_{D_h} = (\rho_h V_h D_h) / \mu_h$	4.16×10^3
$Re_w = (\rho_h V_h r_0) / \mu_h$	4.06×10^5
$Re_\phi = \rho_h \omega r_0^2 / \mu_h$	7.56×10^5
$Re_w / Re_\phi = V_h / (\omega r_0)$	0.538

Governing Equations

Large-Eddy Simulation (LES)

Spatially filtered unsteady 3-D

- Continuity
- Species
- momentum (Navier-Stokes)
- energy

closed by

- thermally perfect gas
- temperature-dependent properties
- WALE turbulence model

Soret and Dufour effects neglected

Reynolds-Averaged Navier-Stokes (steady RANS)

Reynolds averaged 3-D

- Continuity
- Species
- momentum (Navier-Stokes)
- Energy

closed by

- thermally perfect gas
- temperature-dependent properties
- RANS SST model

Soret and Dufour effects neglected

Numerical Method of Solution

LES

Code: ANSYS Fluent v22.1

Algorithm for RI Ingress: SIMPLE scheme (not PISO because...)

- **Time Derivative:** Bounded Second Order Implicit Scheme
- **Spatial Derivatives:** PRESTO for Pressure Interpolation, 2nd-order central for all advection and diffusion terms

Algorithm for EI Ingress: Coupled scheme

- **Time Derivative:** Bounded Second Order Implicit Scheme
- **Spatial Derivatives:** 2nd-order central for all advection and diffusion terms

Time-Step Size & Grid (details given in V&V):

- $\Delta t = 10^{-6} \text{ s} - 10^{-5} \text{ s}$
- $\Delta r^+ = 10 - 30$, $\Delta z^+ = 10 - 30$, $r\Delta\theta^+ = 10 - 30$
- $y^+ < 1$ next to walls

Convergence Criteria:

- At the end of each time step, residuals for continuity $< 10^{-6}$, momentum $< 10^{-7}$, energy $< 10^{-8}$ and CO₂ concentration $< 10^{-8}$ (typically, 40-60 iterations per timestep are needed)

Steady RANS

Code: ANSYS Fluent v22.1

Algorithm : Coupled scheme

- **Spatial Derivatives:** 2nd-order central for all advection and diffusion terms

Grid:

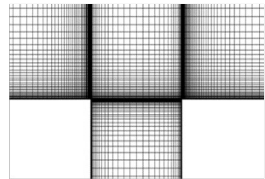
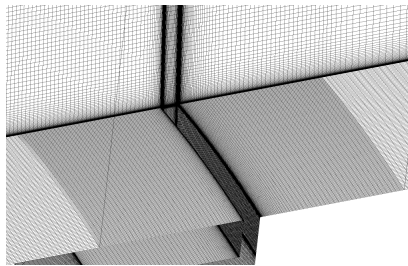
- $y^+ < 1$ next to walls, at least 5 grid points within a $y^+ = 5$

Convergence Criteria:

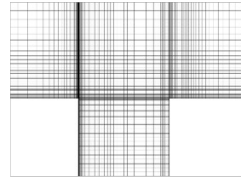
- Residuals for continuity $< 10^{-6}$, momentum $< 10^{-7}$, energy $< 10^{-8}$, and CO₂ concentration $< 10^{-8}$

Verification and Validation

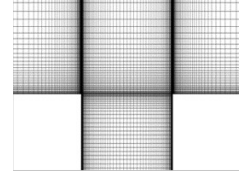
Sector Size
Grid Sensitivity
Time-step Size
Validation



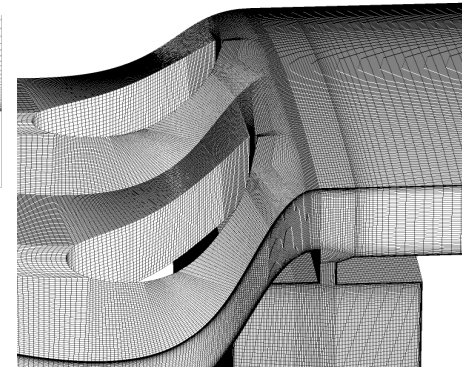
Coarse Grid
10,886,487 nodes
(41 across seal x 101 over 10°)



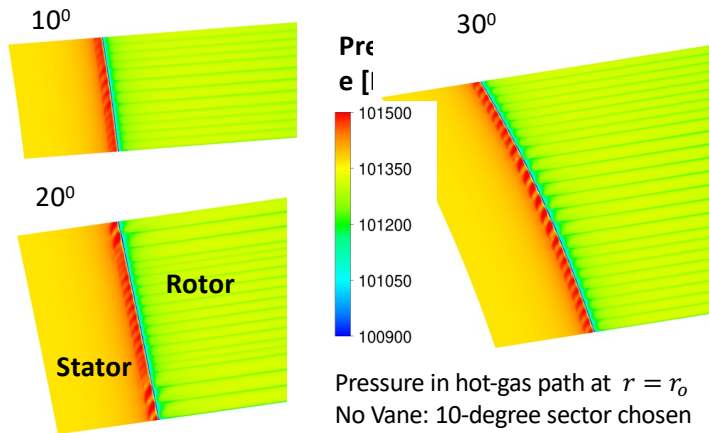
Baseline Grid
11,528,342 nodes
(61 x 101)



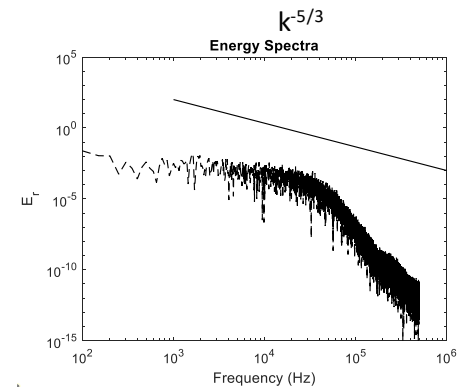
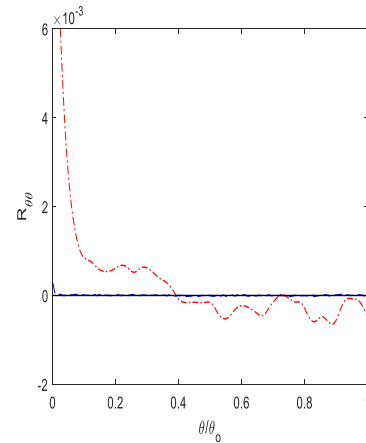
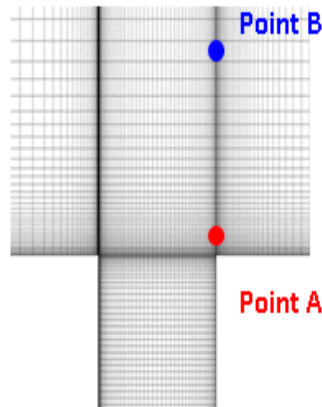
Fine Grid
23,052,782 nodes
(81 x 201)



No Vanes - Sector Size: pressure via RANS SST



LES: 2-Point Correlation in P across 10° Sector

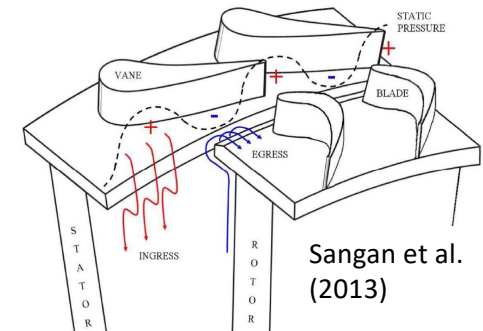


LES: Celik Criteria > 0.9

Key Findings and Gaps in Understanding

Overall:

- Ingress is induced by: (1) rotor disk and its rotation; (2) the pressure variation about the stator vanes' trailing edges, and (3) stagnation pressure induced by the rotor blades.
- Generating **benchmark quality experimental data** that can be used to validate CFD (Green et al. (2014). at OSU, Sangan et al. (2013) at Bath).
- If $Re_w/Re_\phi \ll 1 \rightarrow$ RI dominated; if $Re_w/Re_\phi \geq 1 \rightarrow$ EI dominated



RI Ingress

- **Kelvin-Helmholtz instability** identified (Rabs et al. (2009)), **but how KHI affects RI ingress not explained.**
- **Alternating regions of high & low P on rotor-side of rim seal** have been identified (Green et al. (2014)), **but their causes have never been explained (effects of stator vanes is only a part of the answer).**
- **Conflict flow trajectories** in and out of the seal (Bohn et al. 1995, Sangan (2013)).
- RANS cannot predict RI ingress.
- **LES studies done so far used coarse mesh (Gao et al. (2018)).**

EI Ingress

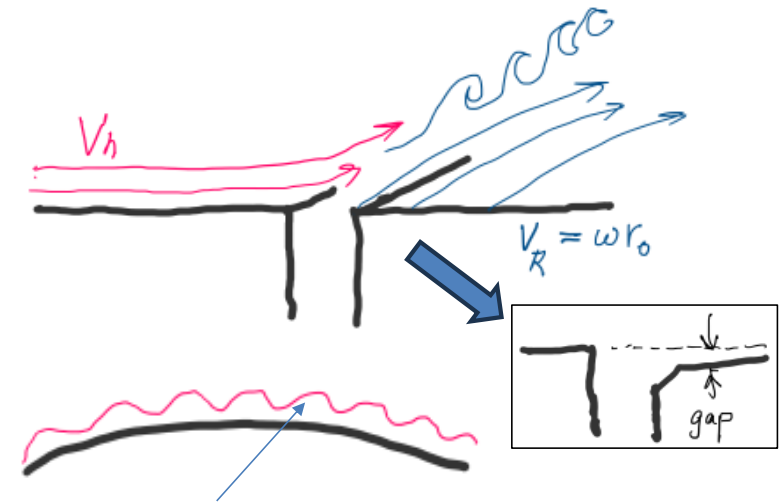
- $C_p = (P - \bar{P}) / (0.5\rho\omega^2 r_o^2)$ is deemed the predictor for EI ingress (Sangan et al. (2013) at Bath), **but want to verify.**
- **Pressure induced by vane dominates ingress (Roy et al. (2001)), but want to understand effect of rotation.**
- RANS cannot predict EI ingress. (Liu et al. (2015))
- **LES studies done so far used coarse mesh. (O'Mahoney et al. (2011))**

RI Ingress for a Configuration w/o Vanes & Blades

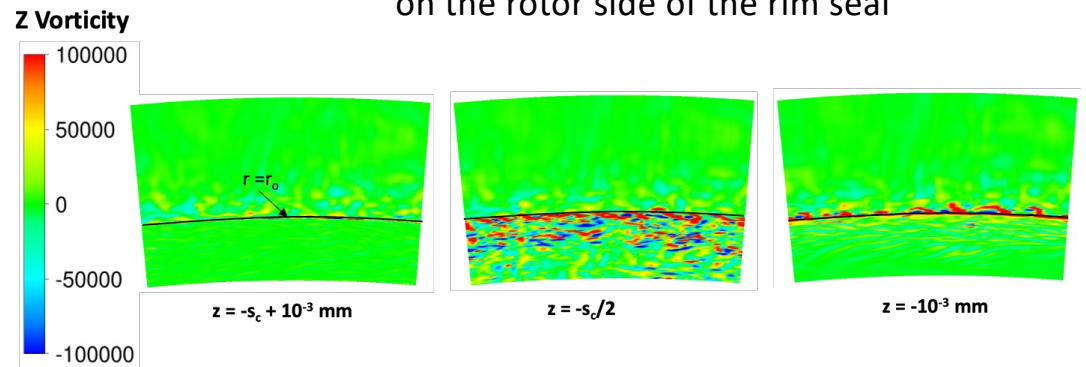
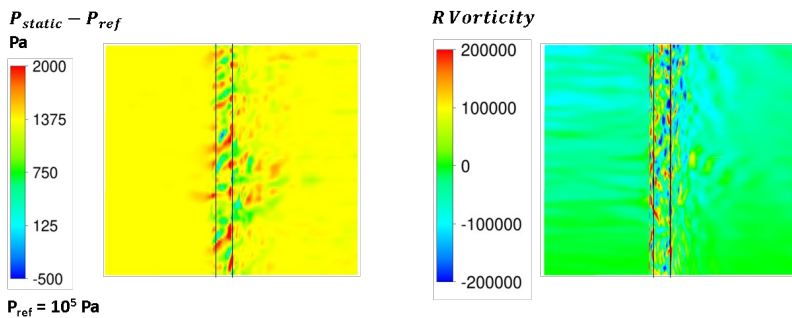
What are the key flow mechanisms?

- Hot-gas flow in axial direction + boundary-layer flow in azimuthal direction about the rotor → Kelvin–Helmholtz instability (KHI).
- KHI → a wavy boundary layer in the azimuthal direction → wavy displacement thickness.
- Hot gas flow over the seal induces a series of recirculating flows in the seal clearance and causes vortex shedding at the seal's backward-facing step.

The wavy displacement thickness formed by KHI and the impingement of shed vortices on the rotor side of the seal create alternating regions of high and low pressures around the rotor side of the seal.

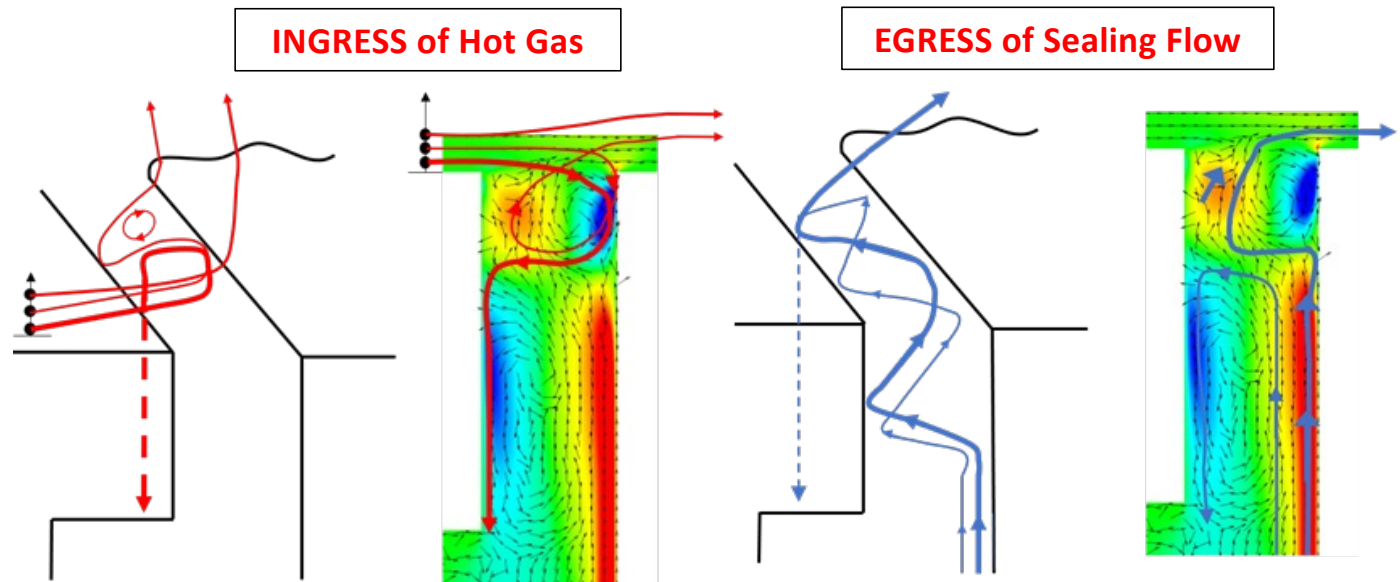
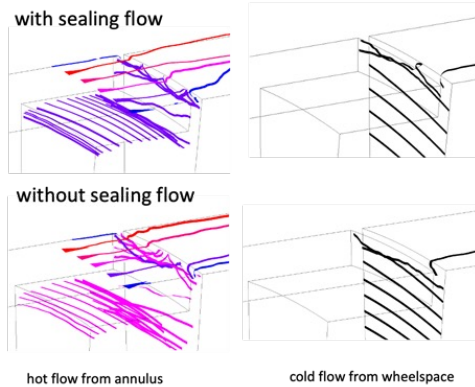


displacement thickness on the rotor side of the rim seal



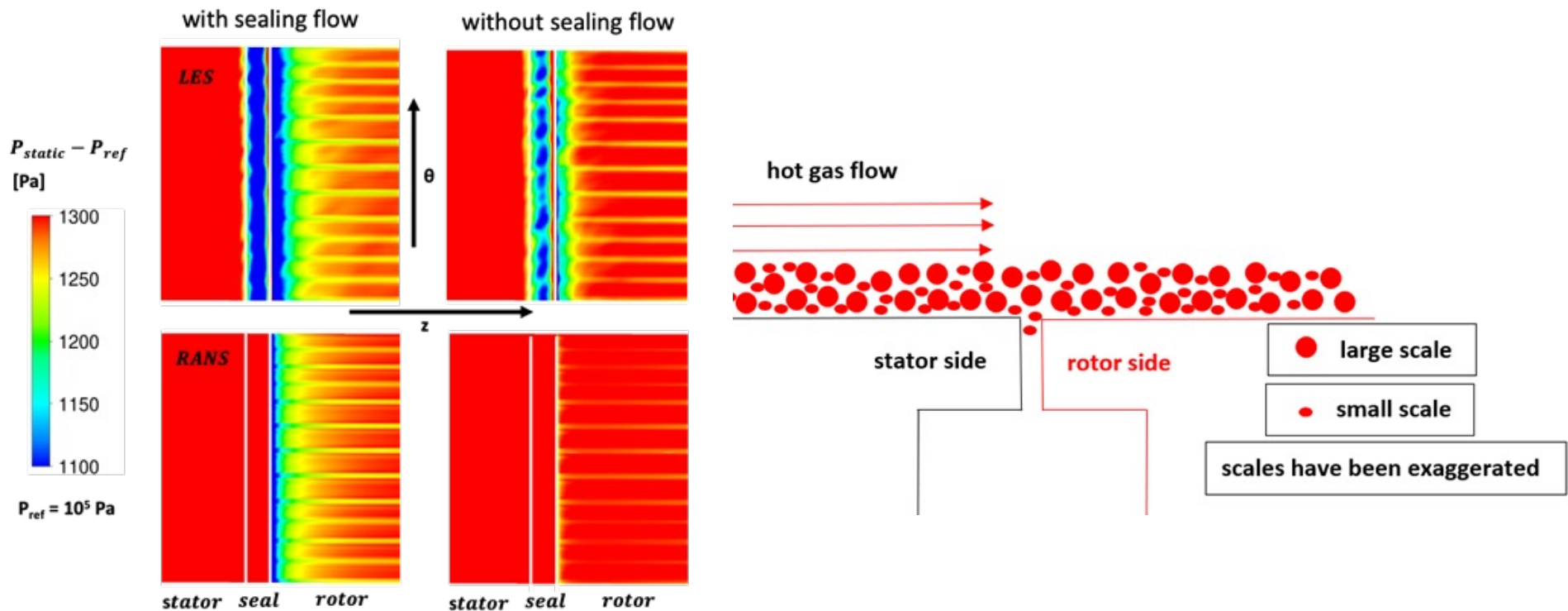
RI Ingress for a Configuration w/o Vanes & Blades

- The alternating regions of high and low pressures cause ingress to start on the rotor side of the seal.
- Regions of high and low pressures around the rotor side of the seal were found to be statistically stationary and do not rotate with the rotor.
- Not all hot gases ingested into the seal reach the wheelspace because the motion induced by the spiraling recirculating flow entrains them back out into the hot gas path.
- On egress, it starts on the rotor side because of “disk pumping” in the wheelspace. However, once reaching the clearance of the seal, it becomes entrained by the recirculating flows there and exits from the stator side.



RI Ingress for a Configuration w/o Vanes & Blades

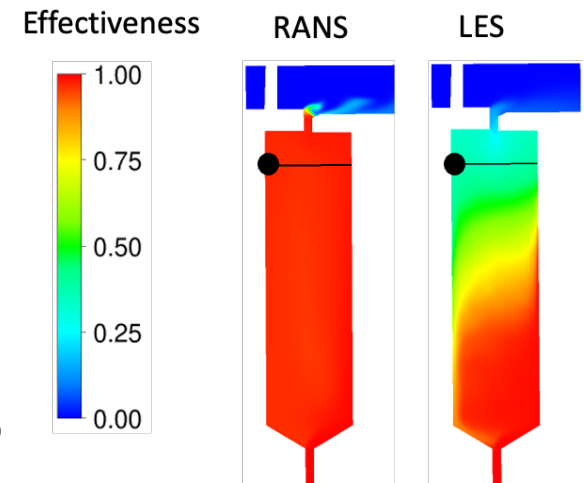
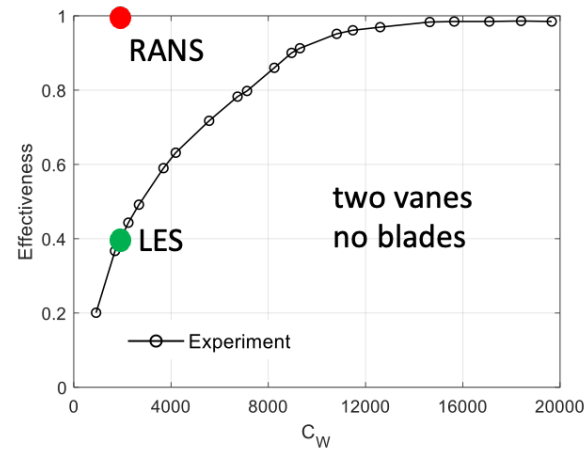
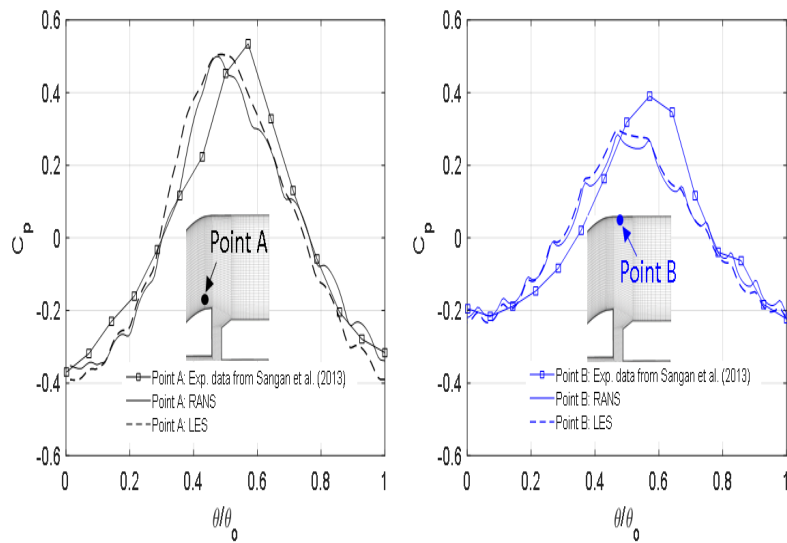
Though RANS with the SST model was able to predict regions of high and low pressures around the rotor side of the seal, it was unable to predict ingress. LES coupled with the WALE model could predict regions of high and low pressures around the rotor side of the seal and the ingress that they create.



EI Ingress for a Configuration with Vanes & No Blades

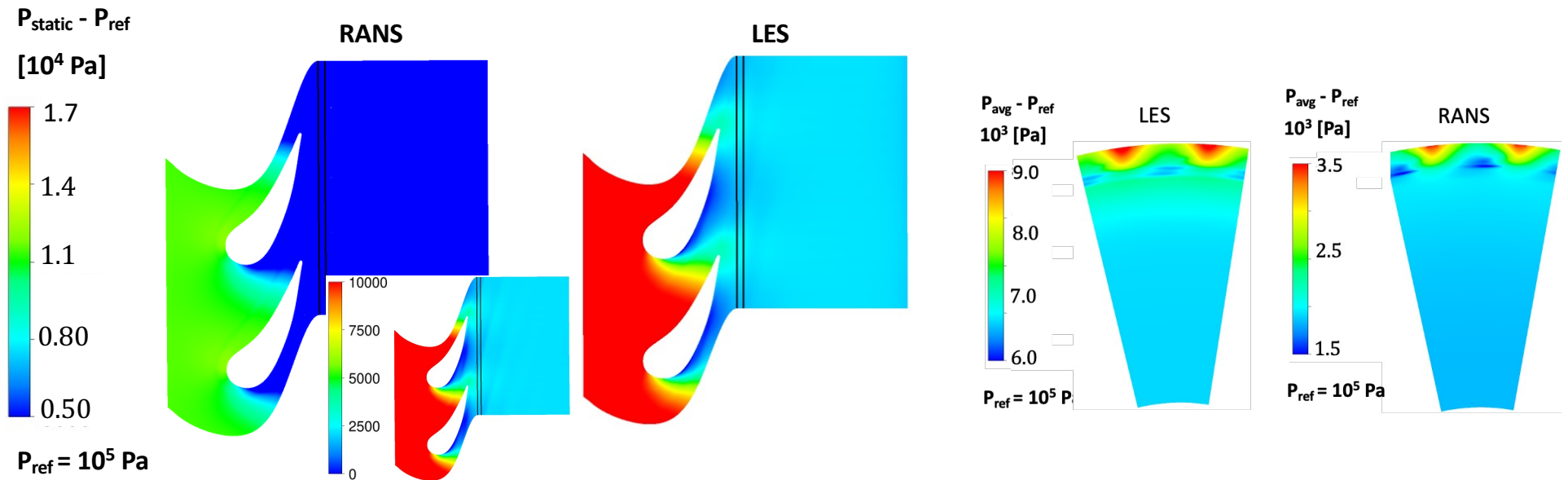
- Both LES and RANS could predict the normalized pressure coefficient, C_p , on the stator platform downstream of the stator vanes and upstream of the seal with reasonable accuracy.
- LES could predict ingress and the correct sealing effectiveness for the configuration and operating condition studied, but RANS could not.

THUS, C_p by itself is inadequate in quantifying ingress.



El Ingress for a Configuration with Vanes & No Blades

- LES predicted a much higher pressure drop in the axial direction about the seal region than RANS, and this produced a much higher pressure drop across the seal in the radial direction to drive ingress into the wheelspace.
- On ingress induced by the stator vanes, it starts in the middle of the seal and later deflects onto the stator side. Once in the wheelspace, the flow is entrained by the vortical structures there.
- On egress, it flows along the rotor side of the wheelspace and exits on the rotor side of the seal.



Our Efforts to Meet Our Nation's Goal of Carbon-Free Generation of Electricity by 2035:

Tools

- Hybrid LES-RANS methods (2 papers in IJNMF - 2021 and 2022)
- ROM for internal cooling passage (2024 IGTI)
- ROM for vane and blade w/ internal and film cooling
- ROM + Optimization + machine learning for design

Fundamentals

- Revisit $T_{\text{adiabatic}}$ on its physical meaning & how to measure.
- Scaling lab to engine conditions: (1) high heating loads (T_w/T_b bear 1 in labs to T_w/T_b up to 2 in engines) and (2) rotation
- Revisit film cooling that couple the flow in the cooling passage and the hot-gas flow (2024 IGTI)

Applications

- Ingress/egress through rim seals via RANS & LES (2 papers in Energies)
- Blade-tip leakage in a 1.5 stage turbine via RANS and LES (2024 IGTI)
- Internal cooling w and w/o rotation and taper (2024 IGTI)
- New film-cooling holes: downstream vortex generators, Y-shaped hole
- New film-cooling design paradigms from machine learning

